

Mechanism of glucose intolerance in mice with dominant negative mutation of CEACAM1

So-Young Park, You-Ree Cho, Hyo-Jeong Kim, Eun-Gyoung Hong, Takamasa Higashimori, Sang Jun Lee, Ira J. Goldberg, Gerald I. Shulman, Sonia M. Najjar and Jason K. Kim

Am J Physiol Endocrinol Metab 291:E517-E524, 2006. First published 25 April 2006;
doi:10.1152/ajpendo.00077.2006

You might find this additional info useful...

This article cites 38 articles, 18 of which can be accessed free at:

<http://ajpendo.physiology.org/content/291/3/E517.full.html#ref-list-1>

This article has been cited by 3 other HighWire hosted articles

Lost in Translation

David H. Wasserman, Julio E. Ayala and Owen P. McGuinness
Diabetes, September, 2009; 58 (9): 1947-1950.

[Full Text] [PDF]

Carcinoembryonic Antigen-Related Cell Adhesion Molecule 1 : A Link Between Insulin and Lipid Metabolism

Anthony M. DeAngelis, Garrett Heinrich, Tong Dai, Thomas A. Bowman, Payal R. Patel, Sang Jun Lee, Eun-Gyoung Hong, Dae Young Jung, Anke Assmann, Rohit N. Kulkarni, Jason K. Kim and Sonia M. Najjar

Diabetes 2008; 57 (9): 2296-2303.

[Abstract] [Full Text] [PDF]

Comparison between surrogate indexes of insulin sensitivity and resistance and hyperinsulinemic euglycemic clamp estimates in mice

Sihoon Lee, Ranganath Muniyappa, Xu Yan, Hui Chen, Lilly Q. Yue, Eun-Gyoung Hong, Jason K. Kim and Michael J. Quon

Am J Physiol Endocrinol Metab, February 1, 2008; 294 (2): E261-E270.

[Abstract] [Full Text] [PDF]

Updated information and services including high resolution figures, can be found at:

<http://ajpendo.physiology.org/content/291/3/E517.full.html>

Additional material and information about *AJP - Endocrinology and Metabolism* can be found at:

<http://www.the-aps.org/publications/ajpendo>

This information is current as of October 20, 2011.

Mechanism of glucose intolerance in mice with dominant negative mutation of CEACAM1

So-Young Park,¹ You-Ree Cho,¹ Hyo-Jeong Kim,¹ Eun-Gyoung Hong,^{1,2} Takamasa Higashimori,¹ Sang Jun Lee,³ Ira J. Goldberg,⁴ Gerald I. Shulman,^{1,5} Sonia M. Najjar,³ and Jason K. Kim^{1,2,5}

¹Department of Internal Medicine, Section of Endocrinology and Metabolism, Yale University School of Medicine, New Haven, Connecticut; ²Department of Cellular and Molecular Physiology, Pennsylvania State University College of Medicine, Hershey, Pennsylvania; ³Department of Pharmacology, Cardiovascular Biology and Metabolic Diseases, Medical University of Ohio, Toledo, Ohio; ⁴Department of Medicine, Columbia University Medical Center, New York, New York; and ⁵Yale Mouse Metabolic Phenotyping Center, Yale University School of Medicine, New Haven, Connecticut

Submitted 16 February 2006; accepted in final form 18 April 2006

Park, So-Young, You-Ree Cho, Hyo-Jeong Kim, Eun-Gyoung Hong, Takamasa Higashimori, Sang Jun Lee, Ira J. Goldberg, Gerald I. Shulman, Sonia M. Najjar, and Jason K. Kim. Mechanism of glucose intolerance in mice with dominant negative mutation of CEACAM1. *Am J Physiol Endocrinol Metab* 291: E517–E524, 2006. First published April 25, 2006; doi:10.1152/ajpendo.00077.2006.—Mice with liver-specific overexpression of dominant negative phosphorylation-defective S503A-CEACAM1 mutant (L-SACCC1) developed chronic hyperinsulinemia resulting from blunted hepatic clearance of insulin, visceral obesity, and glucose intolerance. To determine the underlying mechanism of altered glucose homeostasis, a 2-h hyperinsulinemic euglycemic clamp was performed, and tissue-specific glucose and lipid metabolism was assessed in awake L-SACCC1 and wild-type mice. Inactivation of carcinoembryonic antigen-related cell adhesion molecule 1 (CEACAM1) caused insulin resistance in liver that was mostly due to increased expression of fatty acid synthase and lipid metabolism, resulting in elevated intrahepatic levels of triglyceride and long-chain acyl-CoAs. Whole body insulin resistance in the L-SACCC1 mice was further attributed to defects in insulin-stimulated glucose uptake in skeletal muscle and adipose tissue. Insulin resistance in peripheral tissues was associated with significantly elevated intramuscular fat contents that may be secondary to increased whole body adiposity (assessed by ¹H-MRS) in the L-SACCC1 mice. Overall, these results demonstrate that L-SACCC1 is a mouse model in which chronic hyperinsulinemia acts as a cause, and not a consequence, of insulin resistance. Our findings further indicate the important role of CEACAM1 and hepatic insulin clearance in the pathogenesis of obesity and insulin resistance.

insulin clearance; insulin resistance; skeletal muscle; liver; lipid metabolism

THE PREVALENCE OF OBESITY has reached epidemic proportions in the Westernized countries and is a major factor for the recent dramatic increase in incidence of type 2 diabetes throughout the world (29, 33). Insulin resistance is a major characteristic and requisite event in the development of type 2 diabetes, and a wealth of previous studies (1, 5, 12, 21, 24) has shown that obese humans, as well as genetically or experimentally-induced obese animals, developed insulin resistance in skeletal muscle, adipose tissue, and liver. The mechanism underlying obesity-mediated insulin resistance involves tissue-specific accumulation of fat and fatty acid metabolites and their deleterious effects on insulin signaling and glucose transport activity (2, 20, 34). Additionally, adipocytes produce a host of metabolic hormones and inflammatory cytokines, including resistin, adiponectin, leptin, tumor necrosis factor- α , and interleukin-6, and dysregulated production of these factors has been shown to alter whole body insulin sensitivity (10, 13–15, 37, 40).

The carcinoembryonic antigen-related cell adhesion molecule 1 (CEACAM1) is a transmembrane glycoprotein expressed in various cell types, including endothelial and epithelial cells and B and T lymphocytes, and in the liver among insulin-sensitive organs (32, 39). CEACAM1 is a substrate of the insulin receptor tyrosine kinase and a regulator of receptor-mediated endocytosis and degradation of insulin in liver (25, 35). The physiological role of CEACAM1 in the metabolic regulation has been demonstrated using mice with liver-specific overexpression of dominant negative phosphorylation-defective S503A-CEACAM1 mutant (L-SACCC1 mice) that developed a significant defect in hepatic insulin clearance and subsequent hyperinsulinemia (30). Interestingly, L-SACCC1 mice developed increased visceral adiposity and glucose intolerance (30). Although the circulating leptin levels were normal, L-SACCC1 mice exhibited elevated free fatty acid (FFA) levels, and inhibition of lipolysis with nicotinic acid restored hepatic insulin sensitivity (4). To determine the underlying mechanism of altered glucose homeostasis, tissue-specific insulin action and glucose metabolism were examined during a 2-h hyperinsulinemic euglycemic clamp in awake L-SACCC1 and wild-type mice.

MATERIALS AND METHODS

Animals and surgery. Male L-SACCC1 mice and wild-type littermates were obtained from the animal facility of the Medical University of Ohio at Toledo at 8–10 wk of age (30). Upon arrival, mice were housed in the animal facility of Yale Mouse Metabolic Phenotyping Center for 5–6 wk before the metabolic studies. Mice were housed under controlled temperature (23°C) and lighting [12:12-h light (0700–1900)-dark (1900–0700) cycle] with free access to standard mouse chow diet (6% fat by calories; Harlan Teklad, Madison, WI) and water. At least 4 days before the in vivo experiments, whole body fat and lean mass were measured in awake mice by using ¹H-MRS (magnetic resonance spectroscopy, Bruker Mini-Spec Analyzer; Echo Medical Systems, Houston, TX). Following the body

Address for reprint requests and other correspondence: J. K. Kim, Pennsylvania State University College of Medicine, Dept. of Cellular and Molecular Physiology, 500 Univ. Drive (H166), C4600D, Hershey, PA 17033–0850 (e-mail: jason.kim@psu.edu).

The costs of publication of this article were defrayed in part by the payment of page charges. The article must therefore be hereby marked “advertisement” in accordance with 18 U.S.C. Section 1734 solely to indicate this fact.

composition measurement, mice were anesthetized with an intraperitoneal injection of ketamine (100 mg/kg body wt) and xylazine (10 mg/kg body wt), and an indwelling catheter was inserted in the right internal jugular vein. On the day of clamp experiment, a three-way connector was attached to the catheter to intravenously deliver solutions (e.g., glucose, insulin). Also, mice were placed in a rat-size restrainer (to minimize stress during experiments in the awake state) and tail-restrained using a tape to obtain blood samples from tail vessels. All procedures were approved by the Yale University Animal Care and Use Committee.

Hyperinsulinemic euglycemic clamps to assess insulin action in vivo. Following an overnight fast (~15 h), a 2-h hyperinsulinemic euglycemic clamp was conducted in awake L-SACC1 and wild-type mice ($n = 11-12$), with a primed (150 mU/kg body wt) and continuous infusion of human regular insulin (Humulin; Eli Lilly, Indianapolis, IN) at a rate of 15 pmol·kg⁻¹·min⁻¹ to raise plasma insulin within a physiological range (~300 pM). Blood samples (20 µl) were collected at 20-min intervals for the immediate measurement of plasma glucose concentration, and 20% glucose was infused at variable rates to maintain euglycemia. Basal and insulin-stimulated whole body glucose turnover was estimated with a continuous infusion of [3-³H]glucose (PerkinElmer Life and Analytical Sciences, Boston, MA) for 2 h prior to (0.05 µCi/min) and throughout the clamps (0.1 µCi/min), respectively. All infusions were performed using the microdialysis pumps (CMA/Microdialysis, North Chelmsford, MA). To estimate insulin-stimulated glucose uptake in individual tissues, 2-deoxy-D-[1-¹⁴C]glucose (2-[¹⁴C]DG) was administered as a bolus (10 µCi) at 75 min after the start of clamps. Blood samples were taken before, during, and at the end of clamps for the measurement of plasma [³H]glucose, ³H₂O, 2-[¹⁴C]DG, and/or insulin concentrations. At the end of clamps, mice were anesthetized, and tissues were taken for biochemical and molecular analysis (15).

Biochemical assays. Glucose concentrations during clamps were analyzed using 10 µl of plasma by a glucose oxidase method on Beckman Glucose Analyzer 2 (Beckman, Fullerton, CA). Plasma insulin concentrations were measured by radioimmunoassay using kits from Linco Research (St. Charles, MO). Plasma concentrations of [3-³H]glucose, 2-[¹⁴C]DG, and ³H₂O were determined following deproteinization of plasma samples, as previously described (15). The radioactivity of ³H in tissue glycogen was determined by digesting tissue samples in KOH and precipitating glycogen with ethanol. For the determination of tissue 2-[¹⁴C]DG-6-phosphate (2-[¹⁴C]DG-6-P) content, tissue samples were homogenized, and the supernatants were subjected to an ion exchange column to separate 2-[¹⁴C]DG-6-P from 2-[¹⁴C]DG. Tissue-specific triglyceride concentrations were determined by digesting tissue samples in chloroform-methanol (16). Briefly, the lipid layer was separated using H₂SO₄, and concentrations were determined using triglyceride assay kit (Sigma Diagnostics, St Louis, MO) and spectrophotometry. In additional overnight fasted male L-SACC1 and wild-type mice at 3 mo of age, blood was drawn to determine serum β-hydroxybutyrate levels by gas chromatography/mass spectroscopy following ethyl acetate/diethyl ether extraction of plasma deproteinized with 7% perchloric acid (4).

Calculation. Rates of basal hepatic glucose production (HGP) and insulin-stimulated whole body glucose uptake were determined as the ratio of the [³H]glucose infusion rate (disintegrations/min) to the specific activity of plasma glucose (dpm/µmol) at the end of basal period and during the final 30 min of clamp, respectively. Insulin-stimulated rate of HGP during clamp was determined by subtracting the glucose infusion rate from whole body glucose uptake. Whole body glycolysis was calculated from the rate of increase in plasma ³H₂O concentration, determined by linear regression of the measurements at 80, 90, 100, 110, and 120 min of clamps. Whole body glycogen plus lipid synthesis from glucose was estimated by subtracting whole body glycolysis from whole body glucose uptake (15). Because 2-deoxyglucose is a glucose analog that is phosphorylated but not further metabolized, insulin-stimulated glucose uptake in

individual tissues can be estimated by determining the tissue (i.e., skeletal muscle, adipose tissue) content of 2-[¹⁴C]DG-6-P. On the basis of this, glucose uptake in individual tissues was calculated from plasma 2-[¹⁴C]DG profile, which was fitted with a double exponential or linear curve by using MLAB (Civilized Software, Bethesda, MD) and tissue 2-[¹⁴C]DG-6-P content. Skeletal muscle glycogen synthesis was calculated from ³H incorporation to muscle glycogen, and skeletal muscle glycolysis was estimated as the difference between muscle glucose uptake and muscle glycogen synthesis (15).

Intracellular levels of glucose 6-phosphate and coenzyme A ester. For the measurement of postprandial intracellular concentrations of glucose 6-phosphate (G-6-P), liver was removed from L-SACC1 and wild-type mice at 3 mo of age and immediately frozen using liquid N₂. One gram of tissue was homogenized, resuspended in 5 ml of 6 N perchloric acid, and centrifuged (3,000 g for 10 min at 4°C). The pH of the supernatant was adjusted to 3.5, placed on ice, and mixed with 0.2 M triethanolamine buffer, 0.2 mM NADP, and 5 mM MgCl₂ before 170 U/l G-6-P-dehydrogenase was added. Absorbance was measured at 340 nm before and after the addition of enzyme, and G-6-P content was calculated in µmol/g tissue (4). For the intracellular coenzyme A (CoA) ester levels, 100–200 mg of liver samples were added to an ice-cold mortar and pestle containing 1.5 ml of 6% perchloric acid and homogenized. The homogenate was centrifuged (2,000 g for 10 min at 4°C), 50 µl of 0.32 M dithiothreitol were added to the supernatant, and CoA esters were measured using a modified HPLC procedure (4).

Hepatic glycogen content. Liver samples were obtained at 0800 (postprandial state) or at 1700 (steady state) from age-matched 3-month-old male L-SACC1 and wild-type mice. Frozen tissue samples (20–30 mg) were digested in 1 N NaOH for 2 h at 65°C. Homogenates were centrifuged at 14,000 rpm, and supernatants were spotted on Whatman filter paper. After papers were washed in 70% ethanol, samples were incubated in 0.2 M sodium acetate-amyloglucosidase for 4 h. Afterwards, glucose trinder (Sigma) was added, and samples were incubated at room temperature for 15 min, analyzed at A₅₀₅ nm, and converted to milligrams glycogen per gram of wet tissue weight.

Lipoprotein lipase activity. Following an overnight fast, plasma samples were collected from the age-matched 3-month-old male L-SACC1 and wild-type mice following intravenous injection of heparin (100 IU/kg body wt) via tail vein. Samples (5 µl) were diluted in water and incubated for 60 min at 25°C shaking water bath in 180 µl of incubation medium {10 µl of substrate emulsion containing 10% intralipid (120 mM triglycerol) into which a trace amount of 14 MBq [³H]triolein was introduced, 10 µl heat-inactivated serum as a source of apolipoprotein C-II, 60 µl of deionized water, and 100 µl of incubation buffer (12% fatty acid free bovine serum albumin, 0.02% standard heparin, 0.2 M NaCl, and 0.3 M Tris·HCl, pH 8.5)}. The reaction was stopped by addition of distilled water (0.5 ml) and 2 ml of isopropanol-heptane-H₂SO₄ (48:48.3:1 vol/vol/vol). Total lipids were extracted and fatty acids separated from triglycerol as follows: after centrifugation (2,000 g for 3 min, 4°C), a sample of the upper phase (800 µl) containing total lipids was transferred to new tubes into which 1 ml alkaline ethanol (ethanol 95%-water-2 M NaOH, 500:475:25 vol/vol/vol) and 3 ml heptane were added. After a second centrifugation, the upper heptane phase containing unhydrolysed triglycerol was discarded. A new extraction was performed with 3 ml of heptane. Finally, an aliquot (800 µl) of the remaining alkaline ethanol phase containing fatty acids was counted. All incubations were performed in triplicate. Lipoprotein lipase (LPL) activity was then calculated in milliunits per milliliter plasma (with 1 mU representing 1 nmol of fatty acids released per min) (7).

Western blotting for fatty acid synthase and fatty acid transport protein-1. To determine the expression levels of fatty acid synthase (FAS) and fatty acid transport protein-1 (FATP-1), proteins in frozen tissues were lysed in 0.5% Triton (20), and 75 µg of lysates were analyzed directly by 6 and 10% SDS-PAGE followed by immunoblotting with polyclonal antibodies against FAS (11) and FATP-1

Table 1. Metabolic parameters of the wild-type and L-SACC1 mice at basal and during a 2-h hyperinsulinemic euglycemic clamp experiment

	n	Body weight, g	Basal Period		Clamp Period	
			Plasma glucose, mM	Plasma insulin, pM†	Plasma glucose, mM	Plasma insulin, pM
Wild type	7–11	22±1	7.3±0.6	31±3	5.2±0.5	369±39
L-SACC1	10–12	27±1*	7.1±0.4	67±10*	5.8±0.3	388±63

Values are means ± SE. L-SACC1, liver-specific overexpression of dominant negative phosphorylation-defective S503A-CEACAM1 mutant. * $P < 0.05$ vs. wild-type mice by Student's t -test; †basal plasma insulin levels were measured in a separate group of age-matched mice following an overnight fast.

(M-100, Santa Cruz Biotechnology), respectively. To normalize the expression levels for the amount of proteins loaded on the gels, proteins were probed with α -actin (Sigma-Aldrich). To quantitate the levels of mRNA and proteins, autoradiograms were scanned on an imaging densitometer (Bio-Rad), and proteins and mRNAs were quantitated with SPECTRA MAX Plus (Molecular Devices) using the SoftMAX Pro Macintosh software program (Molecular Devices).

Statistical analysis. Data are expressed as means ± SE. The significance of the difference in mean values between L-SACC1 mice and wild-type mice was evaluated using Student's t -test. Protein and mRNA data were analyzed with Prism3 software (GraphPad Software) using t -test analysis. P values < 0.05 were considered statistically significant.

RESULTS

Body composition and plasma profiles in L-SACC1 mice. The L-SACC1 mice showed a significant increase in body weight (Table 1) that was attributed to a twofold increase in whole body fat mass, as assessed by $^1\text{H-MRS}$ (Fig. 1A). In contrast, whole body lean mass did not differ between the groups (Fig. 1A). Following an overnight fast, plasma glucose levels were similar, but plasma insulin levels were significantly elevated in the L-SACC1 mice (Table 1).

Hepatic glucose metabolism during hyperinsulinemic euglycemic clamp. To assess organ-specific insulin action and glucose metabolism in vivo, a 2-h hyperinsulinemic euglycemic

clamp was conducted in awake male wild-type and L-SACC1 mice. During the clamps, plasma insulin concentration was raised to ~ 300 pM in both groups of mice while plasma glucose concentration was maintained at 5–6 mM by a variable infusion of glucose in all groups (Table 1). The glucose infusion rate required to maintain euglycemia during clamps increased rapidly in the wild-type mice and reached a steady state within 90 min. In contrast, the steady state glucose infusion rate was significantly lower in the L-SACC1 mice (236 ± 16 vs. 352 ± 10 $\mu\text{mol}\cdot\text{kg}^{-1}\cdot\text{min}^{-1}$ in the wild-type mice; Fig. 1B). This indicates that whole body glucose metabolism in response to insulin was markedly blunted in the L-SACC1 mice, consistent with previously reported glucose intolerance in these mice (30). Whole body insulin resistance was partly attributed to reduced insulin sensitivity in liver. Although basal HGP was not altered, the rates of HGP during insulin clamp were increased more than threefold in the L-SACC1 mice (53 ± 13 vs. 16 ± 10 $\mu\text{mol}\cdot\text{kg}^{-1}\cdot\text{min}^{-1}$ in the wild-type mice; Fig. 1C). This resulted in blunted insulin-mediated suppression of HGP (hepatic insulin resistance) in the L-SACC1 mice (49 ± 8 vs. $83 \pm 9\%$ in wild-type mice; Fig. 1D). Also consistent with elevated HGP, intracellular level of G-6-P in liver during the postprandial state was significantly increased in the L-SACC1 mice (0.34 ± 0.07 vs. 0.19 ± 0.02 $\mu\text{mol/g}$ wet tissue in the wild-type mice; Fig. 2A).

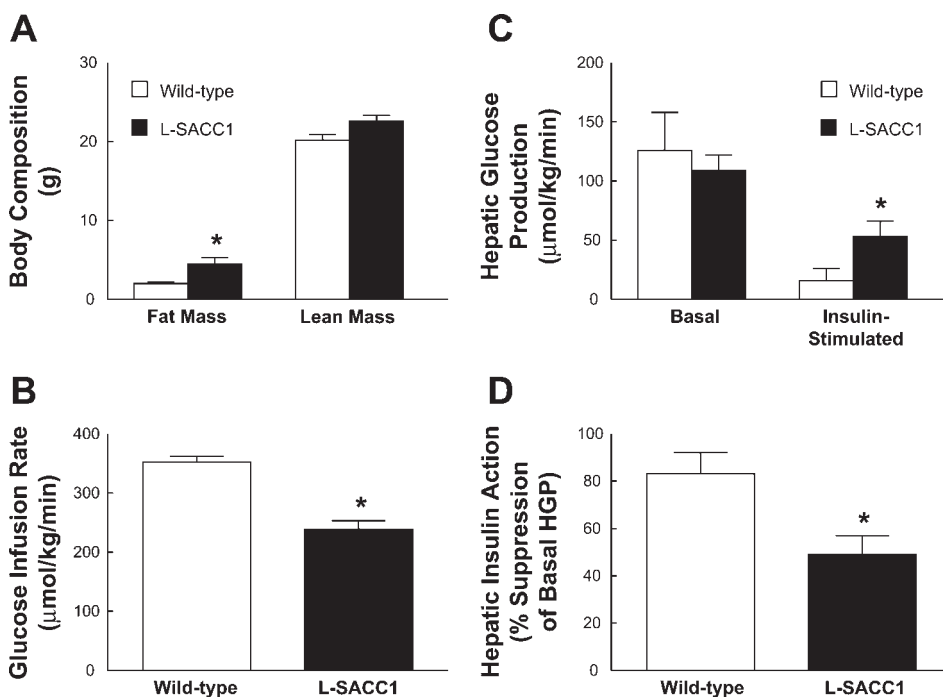
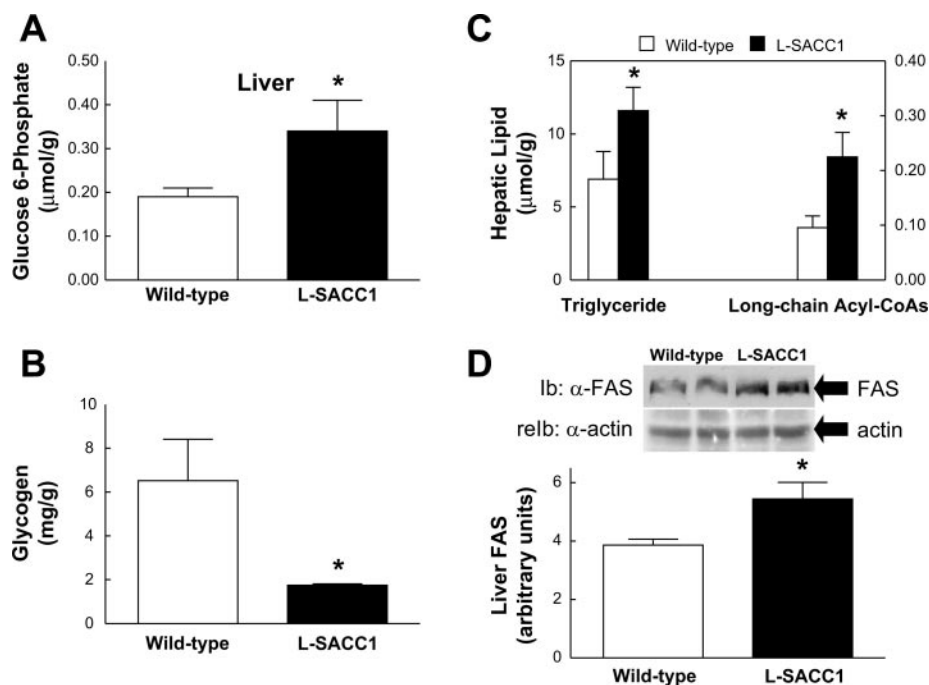


Fig. 1. Body composition and hepatic glucose metabolism in the liver-specific overexpression of dominant negative phosphorylation-defective S503A-CEACAM1 mutant (L-SACC1) mice and wild-type littermates. A: whole body fat and lean mass. B: steady-state glucose infusion rate, obtained from averaged rates of 90–120 min of hyperinsulinemic euglycemic clamps. C: hepatic glucose production (HGP) during basal and insulin-stimulated (clamp) states. D: hepatic insulin action reflected as the %suppression of basal HGP during insulin clamps. Values are means ± SE for 11–12 experiments. * $P < 0.05$ vs. wild-type mice.

Fig. 2. Hepatic glucose and lipid metabolites in the L-SACC1 mice and wild-type littermates. *A*: intracellular glucose 6-phosphate. *B*: intrahepatic glycogen. *C*: intrahepatic triglyceride and long-chain fatty acyl-CoAs. Values are means \pm SE for 5–8 experiments. *D*: hepatic fatty acid synthase (FAS) represented in Western blot and density normalized to actin. Tissue lysates from wild-type and L-SACC1 mice ($n = 5$ for each group, 2 represented blots for each group) were analyzed by SDS-PAGE and immunoblotting with α -FAS antibody followed by reprobing with α -actin to normalize for the amount loaded. * $P < 0.05$ vs. wild-type mice. Ib, immunoblot; reIb, reimmunoblot.



Insulin-mediated suppression of HGP (hepatic insulin action) involves inhibition of gluconeogenesis and stimulation of net hepatic glucose uptake, where the former pathway involves insulin's modulation of phosphoenolpyruvate carboxylkinase (PEPCK) and the latter pathway mostly involves insulin's stimulation of net hepatic glycogen synthesis (5). In this regard, we have previously shown that PEPCK levels were increased in the hepatocytes of L-SACC1 mice (30). Additionally, postprandial hepatic glycogen content was reduced by $\sim 70\%$ in the L-SACC1 mice (1.75 ± 0.10 vs. 6.52 ± 1.89 mg/g wet tissue in the wild-type mice; Fig. 2*B*), suggesting blunted glycogen synthesis.

Hepatic lipid metabolism. In addition to changes in glucose metabolism, hepatic lipid metabolism was altered in the L-SACC1 mice, resulting in a twofold increase in intrahepatic triglyceride content (11.6 ± 1.6 vs. 6.9 ± 1.9 $\mu\text{mol/g}$ in the wild-type mice; Fig. 2*C*, left). This was associated with significant increases in intracellular levels of long-chain fatty acyl-CoAs (0.225 ± 0.045 vs. 0.095 ± 0.021 $\mu\text{mol/g}$ dry wt in the wild-type mice; Fig. 2*C*, right) and protein content of FAS, a key enzyme in de novo lipogenesis, in the liver of L-SACC1 mice (Fig. 2*D*). These results are consistent with our recent report (26) indicating increased FAS activity in the L-SACC1 mice compared with the wild-type mice. Circulating levels of β -hydroxybutyrate were markedly reduced in male L-SACC1 mice (48 ± 7 vs. 482 ± 148 mM in the wild-type mice, $P < 0.05$), suggesting reduced fatty acid β -oxidation. Furthermore, total and hepatic activity of LPL, a rate-determining enzyme in the hydrolysis of circulating triglyceride (7), was unaltered in the L-SACC1 mice (14.0 ± 4.0 vs. 14.5 ± 3.2 $\mu\text{mol FFA} \cdot \text{mL}^{-1} \cdot \text{h}^{-1}$ for total LPL and 4.6 ± 0.5 vs. 5.2 ± 0.5 $\mu\text{mol FFA} \cdot \text{mL}^{-1} \cdot \text{h}^{-1}$ for hepatic LPL in the wild-type mice). Taken together, these results suggest that increases in hepatic lipogenesis and triglyceride release may be responsible for elevated levels of hepatic and circulating triglyceride levels,

whereas whole body lipolysis may not be significantly altered in the L-SACC1 mice (30).

Whole body and peripheral glucose metabolism. Insulin-stimulated whole body glucose uptake was reduced by $\sim 20\%$ in the L-SACC1 mice (289 ± 7 vs. 356 ± 13 $\mu\text{mol} \cdot \text{kg}^{-1} \cdot \text{min}^{-1}$ in the wild-type mice; Fig. 3*A*), indicating insulin resistance in peripheral tissues. Similarly, insulin-stimulated whole body glycogen plus lipid synthesis was reduced by $\sim 30\%$ (107 ± 17 vs. 155 ± 14 $\mu\text{mol} \cdot \text{kg}^{-1} \cdot \text{min}^{-1}$ in the wild-type mice), but insulin-stimulated glycolysis was unaltered in the L-SACC1 mice (Fig. 3, *B* and *C*). Peripheral insulin resistance was mostly accounted for by an $\sim 40\%$ decrease in insulin-stimulated glucose uptake in the skeletal muscle of L-SACC1 mice (241 ± 28 vs. 382 ± 28 $\text{nmol} \cdot \text{g}^{-1} \cdot \text{min}^{-1}$ in the wild-type mice; Fig. 4*A*). Insulin-stimulated glycolysis in skeletal muscle was decreased by $\sim 40\%$ in the L-SACC1 mice (227 ± 28 vs. 370 ± 29 $\text{nmol} \cdot \text{g}^{-1} \cdot \text{min}^{-1}$ in the wild-type mice), whereas glycogen synthesis was unaltered (Fig. 4*B*). Reduced muscle glycolysis despite a normal rate of whole body glycolysis in the L-SACC1 mice suggests that organs other than skeletal muscle may have altered glycolysis. Skeletal muscle insulin resistance was associated with a more than twofold increase in intramuscular triglyceride levels in the L-SACC1 mice (10.2 ± 2.7 vs. 4.1 ± 2.0 $\mu\text{mol/g}$ in the wild-type mice; Fig. 4*C*). The protein level of FATP-1 was unaltered in the skeletal muscle of L-SACC1 mice (Fig. 4*D*).

Furthermore, insulin-stimulated glucose uptake in white and brown adipose tissues was reduced by 30–50% in the L-SACC1 mice (34 ± 7 vs. 75 ± 13 $\text{nmol} \cdot \text{g}^{-1} \cdot \text{min}^{-1}$ and $2,044 \pm 254$ vs. $3,088 \pm 294$ $\text{nmol} \cdot \text{g}^{-1} \cdot \text{min}^{-1}$ in white and brown adipose tissue of wild-type mice, respectively; Fig. 5, *A* and *B*). In addition to altered glucose metabolism, lipid metabolism in white adipose tissue was enhanced in the L-SACC1 mice, as reflected by significantly elevated expression of FAS and FATP-1 (Fig. 5, *C* and *D*).

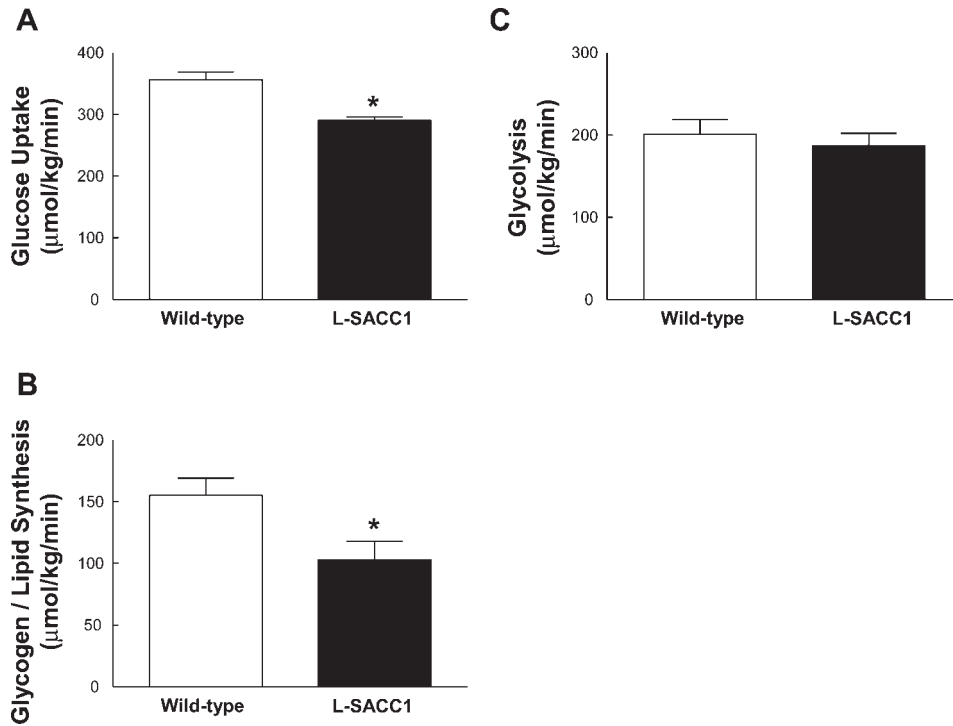


Fig. 3. Insulin-stimulated whole body glucose metabolism in vivo in the L-SACC1 mice and wild-type littermates. *A*: insulin-stimulated whole body glucose uptake. *B*: insulin-stimulated whole body glycogen plus lipid synthesis. *C*: insulin-stimulated whole body glycolysis. Values are means \pm SE for 11–12 experiments. * $P < 0.05$ vs. wild-type mice.

DISCUSSION

We have previously shown that L-SACC1 caused defects in hepatic insulin clearance, chronic hyperinsulinemia, increased visceral adiposity, and glucose intolerance (30). In this study, we performed a hyperinsulinemic euglycemic clamp with labeled glucose to determine the mechanism by which L-SACC1 mice develop altered glucose homeostasis. Our results indicate that L-SACC1 mice are insulin resistant, owing to defects in

hepatic insulin action and insulin-mediated glucose uptake in skeletal muscle and adipose tissue. Insulin resistance in skeletal muscle was associated with increased intramuscular fat content. Insulin resistance in liver and adipose tissue was associated with altered lipid metabolism and elevated expression of genes associated with lipogenesis. Thus our findings indicate that insulin resistance in the L-SACC1 mice is due to altered glucose and lipid metabolism in liver, skeletal muscle, and adipose tissue.

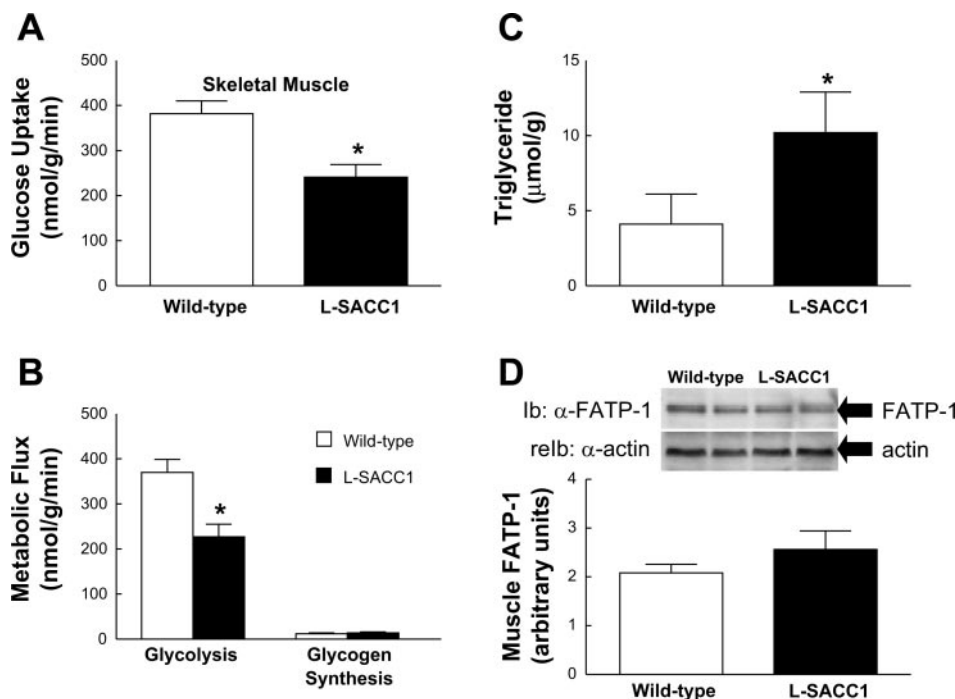
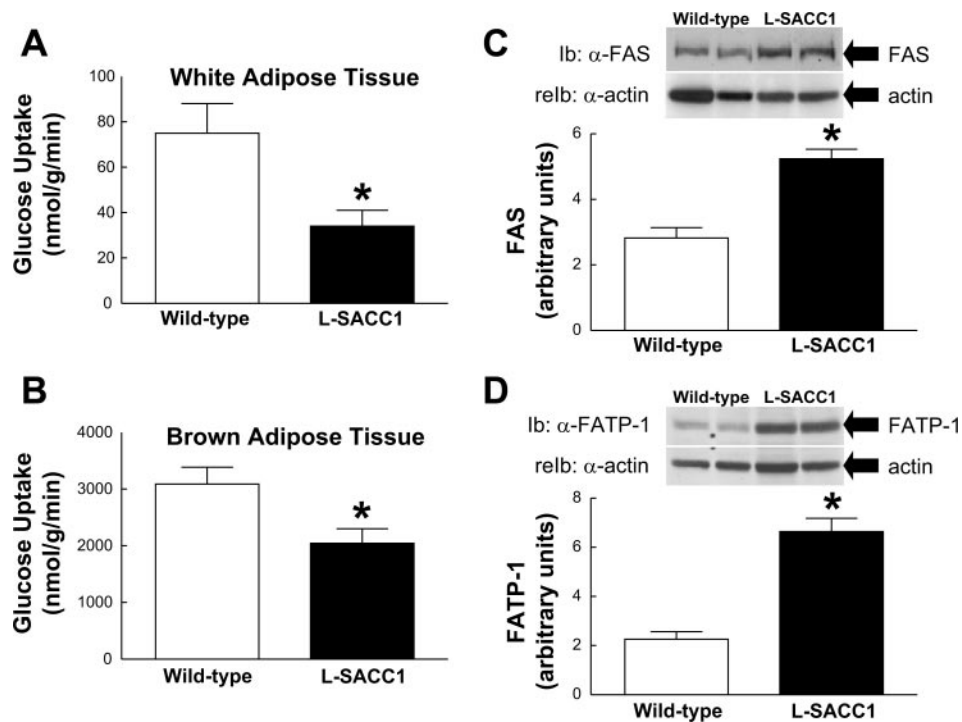


Fig. 4. Glucose metabolism and triglyceride in the skeletal muscle of L-SACC1 mice and wild-type littermates. *A*: insulin-stimulated glucose uptake in skeletal muscle (gastrocnemius). *B*: insulin-stimulated glycolysis and glycogen synthesis in skeletal muscle (gastrocnemius). *C*: intramuscular triglyceride levels (quadriceps). Values are means \pm SE for 11–12 experiments. *D*: skeletal muscle fatty acid transport protein-1 (FATP-1) represented in Western blot and density normalized to actin. Tissue lysates from wild-type and L-SACC1 mice ($n = 5$) were sequentially probed with α -FATP-1 and α -actin antibodies. * $P < 0.05$ vs. wild-type mice.

Fig. 5. Adipose tissue insulin action in L-SACC1 mice and wild-type littermates. *A*: insulin-stimulated glucose uptake in white adipose tissue (epididymal). *B*: insulin-stimulated glucose uptake in brown adipose tissue (interscapular). Values are means \pm SE for 11–12 experiments. *C*: FAS in white adipose tissue represented in Western blot and density normalized to actin ($n = 5$). *D*: FATP-1 in white adipose tissue represented in Western blot and density normalized to actin ($n = 5$). * $P < 0.05$ vs. wild-type mice.



Previous studies have shown that CEACAM1 is required for receptor-mediated insulin endocytosis and that inhibition of its activity impairs hepatic clearance of insulin (3, 6). Recently, we have described a mechanism by which CEACAM1 participates in the transient suppression of hepatic triglyceride synthesis by insulin (26), which arguably counters the lipogenic effect of portal insulin to regulate hepatic triglyceride levels. Our findings of elevated intrahepatic triglyceride and fatty acyl-CoA levels in the L-SACC1 mice further support the regulatory role of CEACAM1 on hepatic lipid metabolism. Additionally, because FAS expression was increased, whereas LPL activity was unaltered in the liver of L-SACC1 mice, increased de novo lipogenesis due to blunted insulin-mediated suppression of proteins associated with lipid metabolism (e.g., FAS) may be responsible for elevated hepatic fat contents (26).

Altered lipid metabolism and intrahepatic accumulation of lipid may be responsible for hepatic insulin resistance in the L-SACC1 mice. Inverse relationship between intracellular fat content and insulin sensitivity has been well documented in studies involving both humans and animal models (23, 22, 38). Increasing fatty acid delivery into liver by overexpressing LPL caused insulin resistance (16), whereas decreasing fatty acid uptake into tissues with the deletion of fatty acid translocase (FAT/CD36) or FATP-1 improved insulin sensitivity (9, 17). The molecular mechanism by which intracellular accumulation of fat causes insulin resistance involves activation of serine kinase cascade, of which PKC θ and/or I κ B kinase- β may play a role, by fatty acid metabolites (i.e., fatty acyl-CoAs, diacylglycerol, ceramide), leading to the serine phosphorylation of insulin receptor substrates (IRS) (8, 18, 28, 41, 42). Subsequent to the serine phosphorylation of IRS, insulin-mediated tyrosine phosphorylation of IRS, activation of phosphatidylinositol 3-kinase and Akt, and GLUT4 translocation are impaired (31). However, because IRS-2 phosphorylation was unaltered in the liver of L-SACC1 mice (30), lipid-mediated alteration of other

IRS isoforms or downstream signaling proteins may mediate hepatic insulin resistance in these mice. Alternatively, hyperinsulinemia-mediated downregulation of insulin receptor in liver may play a role in the pathogenesis of hepatic insulin resistance in the L-SACC1 mice (30).

In addition to altered hepatic glucose and lipid metabolism, L-SACC1 mice developed a profound increase in visceral adiposity in association with altered lipid metabolism in adipocytes and chronic hyperinsulinemia (30). Our previous study showed that mice with muscle-specific deletion of insulin receptor (MIRKO) developed insulin resistance and hyperinsulinemia and elevated whole body fat mass (19). Selective insulin resistance in the skeletal muscle caused hyperinsulinemia-mediated redistribution of substrates to adipose tissue, leading to increased adiposity in the MIRKO mice (19). Our findings of elevated expression of FAS and FATP-1 in the adipocytes of L-SACC1 mice further support increased lipid flux and de novo lipogenesis, possibly due to hyperinsulinemia in these mice (36). In this regard, increased circulating levels of fatty acids directed from adipocytes may further contribute to elevated fat contents and insulin resistance in the liver of L-SACC1 mice. In support of this notion, we have recently shown that reduction of visceral obesity and nicotinic acid-mediated inhibition of lipolysis ameliorated hepatic insulin resistance in the L-SACC1 mice (4).

Although the genetic mutation was directed to a liver-specific protein, CEACAM1, it was surprising to find severe insulin resistance in the skeletal muscle of L-SACC1 mice. In this regard, increased visceral adiposity is also likely to mediate blunted glucose metabolism in skeletal muscle. Our finding of a more than twofold increase in intramuscular triglyceride content suggests that lipid flux into skeletal muscle was enhanced in response to increased adiposity in the L-SACC1 mice. Intramuscular accumulation of fat and fatty acid-derived metabolites may in turn affect insulin signaling and glucose

metabolism (8, 9, 17, 18, 22, 23, 28, 31, 38, 41, 42). Interestingly, our previous *in vitro* study (30) showed normal insulin-mediated glucose transport in the soleus muscle of 2-mo-old L-SACC1 mice that was associated with unaltered intramuscular triglyceride level in isolated soleus muscle of 8-mo-old L-SACC1 mice. The discrepant findings may be attributed to different experimental setting (*in vivo* vs. *in vitro*), fiber type (type I fiber-consisting soleus muscle vs. mixed fiber-consisting gastrocnemius muscle), and/or age of mice studied (2 and 8 mo vs. 4–5 mo). Nonetheless, the present results clearly indicate that insulin-stimulated glucose metabolism *in vivo* is reduced in the L-SACC1 mice, and this defect may be associated with increased intramuscular fat contents. Moreover, insulin-stimulated glucose uptake in white and brown adipose tissue was also reduced in the L-SACC1 mice, and this is consistent with the effects of diet-induced obesity on adipocyte glucose metabolism (27).

We thus propose the following mechanism by which L-SACC1 mice develop whole body insulin resistance. Inactivation of CEACAM1 may cause hepatic insulin resistance by increasing the expression and activity of lipogenic enzymes and lipogenesis in liver. Subsequent accumulation of intrahepatic fat and fatty acid metabolites may downregulate insulin signaling that leads to defects in glucose metabolism. Additionally, inactivation of CEACAM1 may indirectly cause hepatic insulin resistance by blunting hepatic insulin clearance and altering lipid metabolism in adipose tissue in association with chronic hyperinsulinemia. This event, combined with increased adiposity, may further contribute to intrahepatic accumulation of lipid. Altered lipid metabolism and obesity in the L-SACC1 mice may also be responsible for increased intramuscular fat and insulin resistance in skeletal muscle and adipose tissue. Overall, the demonstration that a distinct CEACAM1-dependent signaling pathway modulates insulin clearance without affecting intracellular signaling proposes a mechanism by which hyperinsulinemia may be a cause, and not a consequence, of insulin resistance. Our findings thus indicate the potential role of CEACAM1 and hepatic insulin clearance in the pathogenesis of obesity and insulin resistance.

ACKNOWLEDGMENTS

We are grateful to Aida Groszmann, Mats Fernstrom, Qusai Al-Share, Tong Dai, and Matthew Poy for technical assistance. We are also grateful to Nicola Longo and Gary D. Lopaschuk for helpful discussions.

S.-Y. Park is currently affiliated with the Department of Physiology, Yeungnam University College of Medicine, Daegu, South Korea.

GRANTS

This study was supported by United States Public Health Service Grants U24-DK-59635 (J. K. Kim and G. I. Shulman), DK-54254 (S. M. Najjar), and DK-57497 (S. M. Najjar). This study was also supported by American Diabetes Association Grants 1-04-RA-47 (J. K. Kim), 7-01-JF-05 (J. K. Kim), and 7-03-RA-70 (S. M. Najjar), and The Robert Leet and Clara Guthrie Patterson Trust Award (J. K. Kim).

REFERENCES

1. Boden G. Obesity, free fatty acids, and insulin resistance. *Curr Opin Endo & Diabetes* 8: 235–239, 2001.
2. Boden G and Shulman GI. Free fatty acids in obesity and type 2 diabetes: defining their role in the development of insulin resistance and beta-cell dysfunction. *Eur J Clin Invest* 32: 14–23, 2002.
3. Choice CV, Howard MJ, Poy MN, Hankin MH, and Najjar SM. Insulin stimulates pp120 endocytosis in cells co-expressing insulin receptors. *J Biol Chem* 273: 22194–22200, 1998.
4. Dai T, Abou-Rjaily GA, Al-Share Q, Yang Y, Fernström MA, DeAngelis AM, Lee AD, Sweetman L, Amato A, Pasquali M, Lopaschuk GD, Erickson SK, and Najjar SM. Interaction between altered insulin, and lipid metabolism in CEACAM1-inactive transgenic mice. *J Biol Chem* 279: 45155–45161, 2004.
5. DeFronzo RA. The triumvirate: beta-cell, muscle, liver. A collusion responsible for NIDDM. *Diabetes* 37: 667–687, 1988.
6. Formisano P, Najjar SA, Gross CN, Philippe N, Oriente F, Kern-Buell CL, Accili D, and Gorden P. Receptor-mediated internalization of insulin. Potential role of pp120/HA4, a substrate of the insulin receptor kinase. *J Biol Chem* 270: 24073–24077, 1995.
7. Goldberg IJ. Lipoprotein lipase, and lipolysis: central roles in lipoprotein metabolism and atherogenesis. *J Lipid Res* 37: 693–707, 1996.
8. Griffin ME, Marcucci MJ, Cline GW, Bell K, Barucci N, Lee D, Goodyear LJ, Kraegen EW, White MF, and Shulman GI. Free fatty acid-induced insulin resistance is associated with activation of protein kinase C theta, and alterations in the insulin signaling cascade. *Diabetes* 48: 1270–1274, 1999.
9. Hajri T, Han XX, Bonen A, and Abumrad NA. Defective fatty acid uptake modulates insulin responsiveness, and metabolic responses to diet in CD36-null mice. *J Clin Invest* 109: 1381–1389, 2002.
10. Hotamisligil GS, Shargill NS, and Spiegelman BM. Adipose expression of tumor necrosis factor- α : direct role in obesity-linked insulin resistance. *Science* 259: 87–91, 1993.
11. Joshi AK and Smith S. Construction of a cDNA encoding the multifunctional animal fatty acid synthase, and expression in *Spodoptera frugiperda* cells using baculoviral vectors. *Biochem J* 296: 143–149, 1993.
12. Kahn CR. Insulin action, diabetogenesis, and the cause of type II diabetes. *Diabetes* 43: 1066–1084, 1994.
13. Kahn CR, Chen L, and Cohen SE. Unraveling the mechanism of action of thiazolidinediones. *J Clin Invest* 106: 1305–1307, 2000.
14. Kern PA, Ranganathan S, Li C, Wood L, and Ranganathan G. Adipose tissue tumor necrosis factor and interleukin-6 expression in human obesity and insulin resistance. *Am J Physiol Endocrinol Metab* 280: E745–E751, 2001.
15. Kim HJ, Higashimori T, Park SY, Choi H, Dong J, Kim YJ, Noh HL, Cho YR, Cline G, Kim YB, and Kim JK. Differential effects of interleukin-6 and -10 on skeletal muscle and liver insulin action *in vivo*. *Diabetes* 53: 1060–1067, 2004.
16. Kim JK, Fillmore JJ, Chen Y, Yu C, Moore IK, Pypaert M, Lutz EP, Kako Y, Velez-Carrasco W, Goldberg IJ, Breslow JL, and Shulman GI. Tissue-specific overexpression of lipoprotein lipase causes tissue-specific insulin resistance. *Proc Natl Acad Sci USA* 98: 7522–7527, 2001.
17. Kim JK, Gimeno RE, Higashimori T, Kim HJ, Choi H, Punreddy S, Mozell RL, Tan G, Stricker-Krongrad A, Hirsch DJ, Fillmore JJ, Liu ZX, Dong J, Cline G, Stahl A, Lodish HF, and Shulman GI. Inactivation of fatty acid transport protein 1 prevents fat-induced insulin resistance in skeletal muscle. *J Clin Invest* 113: 756–763, 2004.
18. Kim JK, Fillmore JJ, Sunshine MJ, Albrecht B, Higashimori T, Kim DW, Liu ZX, Soos TJ, Cline GW, O'Brien WR, Littman DR, and Shulman GI. PKC- θ knockout mice are protected from fat-induced insulin resistance. *J Clin Invest* 114: 823–827, 2004.
19. Kim JK, Michael MD, Previs SF, Peroni OD, Mauvais-Jarvis F, Neschen S, Kahn BB, Kahn CR, and Shulman GI. Redistribution of substrates to adipose tissue in mice with selective insulin resistance in muscle promotes obesity. *J Clin Invest* 105: 1791–1797, 2000.
20. Koyama K, Chen G, Lee Y, and Unger RH. Tissue triglycerides, insulin resistance, and insulin production: implications for hyperinsulinemia of obesity. *Am J Physiol Endocrinol Metab* 273: E708–E713, 1997.
21. Kraegen EW, Cooney GJ, Ye J, and Thompson AL. Triglycerides, fatty acids, and insulin resistance—hyperinsulinemia. *Exp Clin Endocrinol Diabetes* 109: S516–S526, 2001.
22. Kraegen EW, Clark PW, Jenkins AB, Daley EA, Chisholm DJ, and Storlien LH. Development of muscle insulin resistance after liver insulin resistance in high-fat-fed rats. *Diabetes* 40: 1397–1403, 1991.
23. Krssak M, Falk Petersen K, Dresner A, DiPietro L, Vogel SM, Rothman DL, Roden M, and Shulman GI. Intramyocellular lipid concentrations are correlated with insulin sensitivity in humans: a ¹H NMR spectroscopy study. *Diabetologia* 42: 113–116, 1999.
24. McGarry JD. What if Minkowski had been ageusic? An alternative angle on diabetes. *Science* 258: 766–770, 1992.
25. Najjar SM, Philippe N, Suzuki Y, Ignacio GA, Formisano P, Accili D, and Taylor SA. Insulin-stimulated phosphorylation of recombinant

- pp120/HA4, an endogenous substrate of the insulin receptor tyrosine kinase. *Biochemistry* 34: 9341–9349, 1995.
26. **Najjar SM, Yang Y, Fernström MA, Lee SJ, DeAngelis AM, Abou-Rjaily GA, Al-Share QY, Dai D, Miller TA, Ratnam S, Ruch RJ, Smith S, Lin SH, Beauchemin N, and Oyarce AM.** Insulin acutely decreases hepatic fatty acid synthase activity. *Cell Metab* 2: 43–53, 2005.
 27. **Park SY, Kim HJ, Wang S, Higashimori T, Dong J, Kim YJ, Cline G, Li H, Prentki M, Shulman GI, Mitchell GA, and Kim JK.** Hormone-sensitive lipase knockout mice have increased hepatic insulin sensitivity and are protected from short-term diet-induced insulin resistance in skeletal muscle and heart. *Am J Physiol Endocrinol Metab* 289: E30–E39, 2005.
 28. **Pederson TM, Kramer DL, and Rondonone CM.** Serine/threonine phosphorylation of IRS-1 triggers its degradation: possible regulation by tyrosine phosphorylation. *Diabetes* 50: 24–31, 2001.
 29. **Pi-Sunyer FX.** The obesity epidemic: pathophysiology, and consequences of obesity. *Obes Res* 10: 97S–104S, 2002.
 30. **Poy MN, Yang Y, Rezaei K, Fernstrom MA, Lee AD, Kido Y, Erickson SK, and Najjar SM.** CEACAM1 regulates insulin clearance in liver. *Nat Genet* 30: 270–276, 2002.
 31. **Rui L, Aguirre V, Kim JK, Shulman GI, Lee A, Corbould A, Dunaif A, and White MF.** Insulin/IGF-1, and TNF-alpha stimulate phosphorylation of IRS-1 at inhibitory Ser307 via distinct pathways. *J Clin Invest* 107: 181–189, 2001.
 32. **Sadekova S, Lamarche-Vane N, Li X, and Beauchemin N.** The CEACAM1-L glycoprotein associates with the actin cytoskeleton and localizes to cell-cell contact through activation of Rho-like GTPases. *Mol Biol Cell* 11: 65–77, 2000.
 33. **Shaw JE, Zimmet PZ, McCarty D, and de Courten M.** Type 2 diabetes worldwide according to the new classification and criteria. *Diabetes Care* 23, *Supp 2*: B5–B10, 2000.
 34. **Shulman GI.** Cellular mechanisms of insulin resistance. *J Clin Invest* 106: 171–176, 2000.
 35. **Soni P, Lakkis M, Poy MN, Fernstrom MA, and Najjar SM.** The differential effects of pp120 (Ceacam 1) on the mitogenic action of insulin, and insulin-like growth factor 1 are regulated by the nonconserved tyrosine 1316 in the insulin receptor. *Mol Cell Biol* 20: 3896–3905, 2000.
 36. **Stahl A, Evans JG, Pattel S, Hirsch D, and Lodish HF.** Insulin causes fatty acid transport protein translocation and enhanced fatty acid uptake in adipocytes. *Dev Cell* 2: 477–488, 2002.
 37. **Steppan CM, Bailey ST, Bhat S, Brown EJ, Banerjee RR, Wright CM, Patel HR, Ahima RS, and Lazar MA.** The hormone resistin links obesity to diabetes. *Nature* 409: 307–312, 2001.
 38. **Unger RH and Orci L.** Lipoapoptosis: its mechanism and its diseases. *Biochim Biophys Acta* 1585: 202–212, 2002.
 39. **Wagener C and Ergun S.** Angiogenic properties of the carcinoembryonic antigen-related cell adhesion molecule. *Exp Cell Res* 261: 19–24, 2000.
 40. **Yamauchi T, Kamon J, Waki H, Terauchi Y, Kubota N, Hara K, Mori Y, Ide T, Murakami K, and Tsuboyama-Kasaoka N.** The fat-derived hormone adiponectin reverses insulin resistance associated with both lipoatrophy and obesity. *Nat Med* 7: 941–946, 2001.
 41. **Yu C, Chen Y, Cline GW, Zhang D, Zong H, Wang Y, Bergeron R, Kim JK, Cushman SW, Cooney GJ, Atcheson B, White MF, Kraegen EW, and Shulman GI.** Mechanism by which fatty acids inhibit insulin activation of insulin receptor substrate-1 (IRS-1)-associated phosphatidylinositol 3-kinase activity in muscle. *J Biol Chem* 277: 50230–50236, 2002.
 42. **Yuan M, Konstantopoulos N, Lee J, Hansen L, Li ZW, Karin M, and Shoelson SE.** Reversal of obesity- and diet-induced insulin resistance with salicylates or targeted disruption of Ikkbeta. *Science* 293: 1673–1677, 2001.

